2017 IEEE/RSJ International Conference on Intelligent Robots and Systems (IROS)
September 24–28, 2017, Vancouver, BC, Canada

A Glove-based System for Studying Hand-Object Manipulation via Joint Pose and Force Sensing

Hangxin Liu[1⋆] Xu Xie[1⋆] Matt Millar[1⋆] Mark Edmonds[1] Feng Gao[1]
Yixin Zhu[1] Veronica J. Santos[2] Brandon Rothrock[3] Song-Chun Zhu[1]

***Abstract*— We present a design of an easy-to-replicate glove-based system that can reliably perform simultaneous hand pose and force sensing in real time, for the purpose of collecting human hand data during fine manipulative actions. The design consists of a sensory glove that is capable of jointly collecting data of finger poses, hand poses, as well as forces on palm and each phalanx. Specifically, the sensory glove employs a network of 15 IMUs to measure the rotations between individual phalanxes. Hand pose is then reconstructed using forward kinematics. Contact forces on the palm and each phalanx are measured by 6 customized force sensors made from Velostat, a piezoresistive material whose force-voltage relation is investigated. We further develop an open-source software pipeline consisting of drivers and processing code and a system for visualizing hand actions that is compatible with the popular Raspberry Pi architecture. In our experiment, we conduct a series of evaluations that quantitatively characterize both individual sensors and the overall system, proving the effectiveness of the proposed design.**

I. Introduction

Robots that imitate the behaviors of humans may enable more natural and friendly interactions with humans in man-made environments, as with robotic handshaking [1]. Just as whole body sensing [2] is critical for the study of human movement, hand pose and force information is crucial to the investigation of manipulative tasks. While researchers can track hand pose based on perception [3], force estimation from vision using numerical differentiation methods [4], [5], or sophisticated physics-based soft-body simulation [6], [7], glove-based devices still have their own advantages, presenting convenient, integrated solutions that can be natural and essential for collecting ground truth hand data during manipulations and interactions.

Designs of tactile gloves have long been proposed for a wide range of applications, and they remain an active research area. Dipietro *et al.* provided a comprehensive survey of glove-based system designs and their application from 1970s to 2008 [8]. Since then, a number of novel designs have emerged to address existing limitations, including portability, reliability, and cost. As the main motivations of developing data/tactile gloves or other glove-based systems are obtaining the pose and force information during manipulative actions, we divide some notable recent designs since 2008 into two categories based on the types of data they can collect: gloves with i) only pose-sensing, and ii) joint pose- and force-sensing.

(a) (b)

Fig. 1: Prototype consisting of (a) 15 IMUs on the dorsum of the hand and (b) 6 integrated Velostat force sensor with 26 taxels on the palmar aspects of the hand.

Pose sensing gloves generally utilized IMUs, flex sensors, or similar orientation systems to obtain finger joint angles. Taylor *et al.* [9] tests a Zigbee network of IMUs using independent state estimation for feasibility of joint prediction. In the design by Kortier *et al.* , each of 15 phalanxes is fitted with a PCB populated with one 6 degree-of-freedom (DoF) accelerometer/gyroscope and one 3DoF magnetometer. In this way, a more comprehensive representation of the hand pose is captured [10]. Ligorio *et al.* improves localization of the phalanx by combining IMUs with a camera-based localization system [11]. Efforts have been made to improve pose sensing accuracy using filtering [12] and estimation techniques like the extended Kalman filter [10], [11], [13]. Using curvature/flex sensors to measure finger flexion is an approach that has been proven to be effective [14], [15]. This approach, however, may bring discomfort to the user or sacrifice the user's dexterity. Another recent design, Wolverine [16], adapts a DC motor and time-of-flight sensor into an exoskeleton structure in order to obtain hand pose without using a glove directly.

Pose and force sensing glove-based systems represent efforts to combine both force sensing and pose sensing into an integrated system. Hammond *et al.* [17] designs a liquid-metal embedded elastomer sensor that can measure

⋆ H. Liu, X. Xie and M. Millar contributed equally to this work.
[1] UCLA Center for Vision, Cognition, Learning, and Autonomy (VCLA) at Statistics Department. Emails: {hx.liu, xiexu, millar, markedmonds, f.gao, yixin.zhu}@ucla.edu, sczhu@stat.ucla.edu.
[2] Biomechatronics Lab in the UCLA Mechanical and Aerospace Engineering Department. Email: vjsantos@ucla.edu.
[3] Jet Propulsion Laboratory. Email: rothrock@jpl.nasa.gov.

force across the palm. The sensors measure skin strain in order to track joint motion, which may lead to less reliable measurement. In the design by Gu *et al.* [18], a glove equipped with FlexiForce sensors is used to collect force information, and a Vicon motion capture system is employed to track wrist, index finger, and thumb angles for manipulative action recognition. For applications that focus more on the fingertip, a specific tactile sensor is available [19]. Further related work involves estimating manipulative force from hand pose obtained via a network of 9DoF IMUs, *e.g.* [20]. One potential drawback is that many of the commonly-used force sensors such as the FlexForce are built on plastic substrates that, while flexible compared to a standard PCB, can be too rigid to conform to the contours of the hand, resulting in limitations on natural hand motion during fine manipulative actions, particularly when a large force sensing area is desired. In recent years, Velostat, a piezoresistive conductive film, has become popular and is applied to pressure sensing in the fields of soft robotics [21], robotic touch perception [22], robotic tactile interaction [23], and gesture recognition [24].

The aforementioned efforts in the literature, particularly in joint pose/force sensing, indicates the needs for capturing the dynamics and not just the kinematics involved in fine manipulative actions. Such demand is especially important given that changes in hand-object interaction forces are not always accompanied by measurable changes in hand posture. The study of fine hand-object manipulative interactions requires finer spatial resolution force sensing, in combination with pose sensing, than has previously been demonstrated. The objective of this work is to create, characterize, and demonstrate an integrated system that extends pose sensing gloves with force sensing over large areas, with finer spatial resolution, and with materials that do not constrain natural hand motion.

Contributions: The glove-based system presented in this paper makes the following contributions:

1) The proposed design is an easy-to-replicate, cost-effective glove-based system that performs simultaneous hand pose and force sensing in real time for the purpose of studying fine manipulative actions. A configuration of IMUs similar to [10] is adapted and inter-joint rotations are captured in order to reconstruct hand pose with a high degree of comprehensiveness, as shown in Fig. 1a.
2) We design a customized force sensor using Velostat (Fig. 1b), whose force-voltage relation is investigated, in order to capture distributions of forces over large areas of the hand rather than just at single contact points (e.g. fingertips only).
3) All software implementation of the proposed design, including the forward kinematics model for the hand, force vector derivation, and visualization of manipulative actions, are developed using the Robot Operating System (ROS) framework, and are publicly available at *GitHub*.
4) A prototype system is evaluated and characterized, showcasing its capability for reliably capturing dynamical information about manipulative actions. We further analyze the power consumption of the prototype system, indicating it can be powered by a small, portable power bank and be wireless to improve user's mobility.

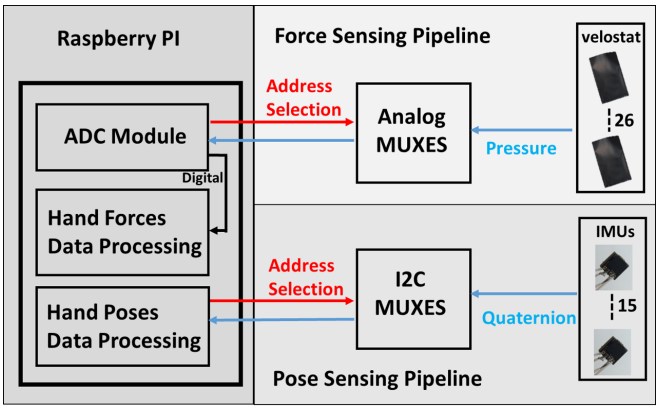

Fig. 2: Overall system schematic

Overview: The remaining sections of the paper are organized as follows. The proposed overall design and hardware implementations of the prototype are described in Section II. This section also details the construction of the Velostat force sensors and its force-voltage relationships. The software implementation consisting of the forward kinematics model of the hand, force vector derivation, and visualization for manipulative actions are shown in Section III. The performance of the proposed design is evaluated in Section IV via a series of experiments.

II. Overall Design and Prototyping

This section presents the overall system schematic. In hardware implementation, a network of 15 IMUs are configured and deployed. For the force sensing pipeline, we utilized Velostat, a piezoresistive conductive film whose resistance changes in response to applied forces, to construct a force sensor that is capable of measuring contact force over a large area via an array of individual taxels. A prototype of the design is built and presented as well.

A. Overall Design

An integrated system consisting of a glove and a processing unit for hand pose and force acquisition is developed. Fig. 2 shows a schematic of the integrated system deploying two sensing networks. A network of 15 IMUs is equipped to measure the orientation of the palm and each phalanx for comprehensive hand pose reconstruction. A network of 6 customized force sensors constructed from a piezoresistive conductive film—Velostat—are attached to the palm and each finger, and contact forces are measured.

B. Hardware Implementation

a) Pose sensing pipeline: The pose estimation module is built from 15 Bosch BNO055 9DoF IMUs. One IMU is mounted to the palm of the glove, twelve are mounted to the three phalanxes on each of the four fingers, and one IMU each is mounted to the distal and intermediate phalanges of the thumb. Each IMU contains a 12-bit triaxial

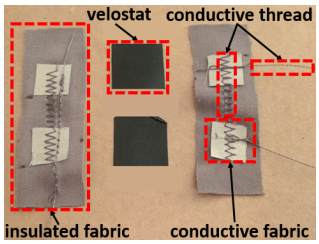

(a) Velostat sensor construction

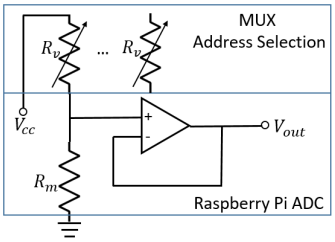

(b) Velostat sensor circuit

Fig. 3: Velostat force sensor construction and circuit layout

accelerometer, a 16-bit triaxial gyroscope, and a triaxial geomagnetometer. Sensor fusion is performed via a proprietary algorithm on a 32-bit microcontroller, yielding a global-frame orientation quaternion for each phalanx of hand.

The BNO055 footprint is 5×4.5 mm^2 and is mounted on a customized 6.35×6.35 mm^2 breakout PCB, making it easier to attach to the glove fabric with minimum constraints on the user's natural hand motion. These sensors are networked over a pair of I^{2}C buses in star configuration, each of which is multiplexed using one TCA9548A I^{2}C multiplexer. Each of these two multiplexers is connected to one of two I^{2}C bus interfaces available on a single Raspberry Pi 2 Model B, which acts as the master controller for the entire glove system. We base the layout for our pose-sensing pipeline largely on work by Kortier *et al.* [10], whose experiments quantify the characteristics of such an arrangement.

Physical connections use a high-flexibility, silicone-coated 29-gauge stranded-core wire. The IMUs are fixed with neutral cure silicone rubber into small 3D-printed housings, which are sewn into the glove's Lycra fabric over the top of their corresponding phalanxes.

b) Force sensing pipeline: The force sensing pipeline uses a network of force sensors deploying Velostat. Fig. 3a shows the multi-layer structure of this sensor. A single-point-sensing version of these sensor is constructed by layering small strips of Velostat (2×2 cm^2) between two outer shells of conductive fabric with conductive thread stitched into it. Lead wires to the pad are braided into the conductive thread fibers. The braided wire is then soldered to itself to form loops that hold the braid in place.

Time division of the channels is done for the palm grid via a pair of 74HC4051 analog multiplexers, and for the pads on the fingers via a single CD74HC4067 analog multiplexer. The multiplexers are controlled via the Raspberry Pi 2's GPIO, and their values are read into the Raspberry Pi via an SPI-enabled ADS1256 ADC at 40 whole-hand sps.

c) Force sensor characterization: In order to characterize the force-voltage relation of the sensor, an experiment is conducted using a similar setup to that mentioned in [25]. Weights are applied to a 2×2 cm^2 Velostat sensing taxel ranging in value from 0.1 kg to 1.0 kg in 0.1 kg increments, and additionally at values of 1.2, 1.5, and 2.0 kg. All Velostat sensors utilized in prototyping are made of the same 2×2 cm^2 size taxel to ensure a single force-voltage relation can be applied. The calibration circuit is the same as Fig. 3b except that only the Velostat taxel of interest is connected. A voltage divider to allow tuning of

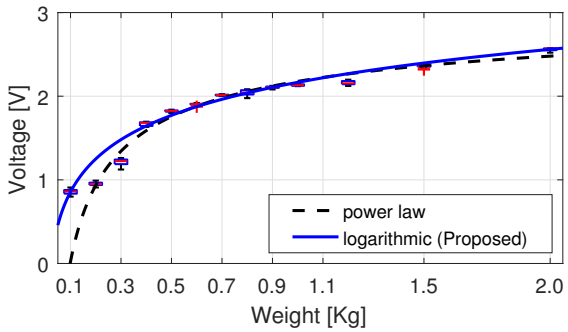

Fig. 4: Force-voltage relation of one constructed Velostat sensing unit. A logarithmic law fit performs better than a power law fit.

the taxel's sensing range was proposed by Lee *et al.* [25], in which the force-voltage relation follows a power law with different coefficients, yielding the force voltage relation $F = -1.067V^{-0.4798} + 3.244$ with $R^2 = 0.9704$, where F is the applied force in terms of weight and V is the output voltage. In this paper, however, we approximate the force-voltage relation with a logarithmic law instead due to its better R^2 value under our experimental setup, which yields the relation $F = 0.569 \log(44.98V)$ with $R^2 = 0.9902$. The comparisons between power law and logmarithmic law are shown in Fig. 4.

C. Prototyping

Fig. 1 shows a prototype of the proposed design and Table I lists the equipment we utilized in the prototype and their parameters. The force sensing functionality is achieved by deploying five 2×1 customized Velostat force sensors on each finger / thumb that each detects pressure in two regions (proximal and distal), and a single 4×4 sensor spreads over the gloves palm. The sensors placements and sensing regions are shown in Fig. 1b. By constructing a voltage divider circuit as shown in Fig. 3b, where multiple Velostat sensors are connected in parallel via a multiplexer that accesses a single sensor at a time. The Analog-to-Digital converter (ADC) extended from the Raspberry Pi integrated with a 200Ω resistor serves as the voltage divider. The resistance of the corresponding cell can be measured to capture the force in that region. This arrangement enables the capability of measuring the force distributed on the hand.

The 15 IMUs on each phalanx and the palm (Fig. 1a) provide pose sensing. These IMUs are connected to the Raspberry Pi 2, a single-board computer that is well suited for wearable devices, via proper multiplexers. With the merit

TABLE I: Prototyping hardware parameters

Parameter	Value
BNO055 IMU	N = 15
Sampling Frequency	20 [Hz]
Velostat sensor	N = 26
Sampling Frequency	40 [Hz]
Raspberry Pi 2	N = 1
Quad-core CPU	900 [MHz]
RAM	1 [GB]

of remote accessing in Raspberry Pi and ROS, one can access the processed data in Raspberry Pi remotely and visualize in workstations.

Compared to the existing expensive commercially available glove-based systems, which are only capable of transmitting raw data collected by the sensors to a workstation, our proposed design can enable on-board processing (see Section III) of the captured information.

D. System Power Analysis

In order to make the entire glove-based system more portable, including the processing unit, we investigate the power consumption of the major components and the system as a whole. The power is calculated by the product of the voltage and current across the components of interest. The results reported in Table II are the peak values over 10 minutes of continuous operation. The proposed system has the merit of low power consumption by having a peak of $2.72W$ in total. Thus, a normal cellphone power bank (5V output, 3.5Ah, and 75g) could power the system for a reasonable amount of operation time. The proposed system can be operated in a fully wireless manner after adding a wireless adapter, improving user's mobility.

III. Software Implementation

In the subsequent subsections, we introduce three core software implementations: i) hand pose calculation, ii) force vector derivation, and iii) manipulative action visualization of both hand pose and hand-object interaction forces. In an effort to maximize compatibility with different usages, the software, including processing and visualization, is built on top of the ROS environment.

A. Hand Pose Reconstruction using Forward Kinematics

Hand forward kinematics: The human hand has approximately 20 degrees-of-freedom (DoF): 2 DoF for metacarpophalangeal (MCP) joints, 1 DoF for proximal interphalangeal (PIP) joints, and 1 DoF for distal interphalangeal (DIP) joints. Using such structure, each finger can be modeled as a 4 DoF kinematic chain where the palm is the base frame and the distal phalanx is the end-effector frame. For simplicity, we model the thumb as a 3 DoF kinematic chain consisting nominally of its interphalangeal and carpometacarpal joints.

Given the rotations measured by two consecutive IMUs, joint angles are obtained and the position and orientation of each phalanx can be computed by forward-kinematics. Fig. 5 shows the frame attachment and the kinematic chain of the index finger as an example. The palm is assigned as Frame 1, the proximal, middle, and distal phalanx are Frame 2 to Frame 4, respectively. l_1, l_2, and l_3 denote the length

TABLE II: Power consumption of the system

Component	Power (W)
IMU ($\times$15) Network with MUX	0.60
Velostat Sensor with MUX	0.02
Raspberry Pi with ADC	2.15
Total	2.72

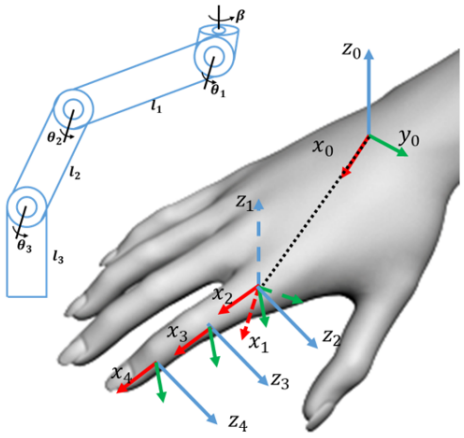

Fig. 5: Frame attachment and the kinematic chain of the index finger, as an example

for proximal, middle, and distal phalanx, respectively. β and θ_1 denote the abduction/adduction and flexion/extension angles of the MCP joint while θ_2 and θ_3 denote the flexion/extension angles of the PIP and DIP joints. d_x and d_y are the offset between palms center to the MCP joint in the x and y directions. Given these notations, the standard Denavit-Hartenberg (D-H) parameters are derived for each reference frame and tabulated in Table III. A general homogeneous transformation matrix T from frame $i-1$ to i is

$$ {}^{i-1}_{i}T = \begin{bmatrix} c\theta_i & -s\theta_i & 0 & a_{i-1} \\ s\theta_i c\alpha_{i-1} & c\theta_i c\alpha_{i-1} & -s\alpha_{i-1} & -s\alpha_{i-1}d_i \\ s\theta_i s\alpha_{i-1} & c\theta_i s\alpha_{i-1} & c\alpha_{i-1} & c\alpha_{i-1}d_i \\ 0 & 0 & 0 & 1 \end{bmatrix}, \quad (1) $$

where $c\theta_i$ denotes $\cos(\theta_i)$ and $s\theta_i$ denotes $\sin(\theta_i)$.

The pose of each phalanx in Cartesian space can be expressed in the palm reference frame by concatenating the homogeneous transformation matrix as shown in Table IV.

Joint limits: A commonly used closed form representation of the finger joints motion constraints [26] is adapted.

$$ 0^\circ \le \theta_1 \le 90^\circ $$
$$ 0^\circ \le \theta_2 \le 110^\circ \quad (2) $$
$$ 0^\circ \le \theta_3 \le 90^\circ $$
$$ -15^\circ \le \beta \le 15^\circ \quad (3) $$

The imposed joint limits define the upper and lower bounds of the joint motions and, thus, eliminate unnatural hand gestures due to sensor noise.

The forward kinematics models also keep track of the potential rotational offset between each fabric-mounted sensor and the underlying bone (skin-motion artifact), which account for two sources of error: i) the process of mounting and sewing the IMUs into the fabric of the glove introduces inconsistencies in the alignment of the sensors with respect to the actual phalanxes, and ii) anatomical differences between users result in IMU mounts naturally falling into places in different configurations dependent on the anthropometry of the user's hand.

Pose calibration: A compensatory calibration routine is performed to further eliminate the aforementioned in-

consistencies. First, the hand is held flat on a table in a canonical pose. A glove-local reference frame is defined with x-y in the plane of the table and the x-axis parallel to the user's middle finger. The orientation of the single IMU on the palm is measured by hand with respect to this glove-local frame, $q_{\text{glove}\to\text{sensor}_{\text{palm}}} \in \mathbb{H}$. Then, a calibration event signal is called, triggering the forward kinematics code to update via direct measurement its internal representation of the rotation $q_{\text{sensor}_{\text{palm}}\to\text{sensor}_i} \in \mathbb{H}$ between the sensor on the palm and each of the remaining 14 sensors. Since the rotation $q_{\text{glove}\to\text{sensor}_{\text{palm}}}$ is already measured, it becomes trivial to compute the rotational errors $q_{\text{glove}\to\text{sensor}_i}$, which can then be cancelled out of the measured orientations.

B. Force Vector Derivation

We further combine force scalar data obtained from the force sensors with our estimated hand pose into the form of force vectors, enabling heterogeneous forces and poses in manipulative actions to share a shared representation. Specifically, each force vector is defined with the magnitude equal to the force reading from the corresponding force sensor. Vector direction is then set to be perpendicular to the finger phalanx that encoded the pose information. Due to the construction of our force sensors, the force reading obtained measures only the pressure but not the stress component of the surface force over the sensing fabric. In general, the force vector to one frame could be expressed as follow:

$$(F_{X_{ref}}, F_{Y_{ref}}, F_{Z_{ref}})^T, \tag{4}$$

where the *ref* denotes the frame we are referring to.

By applying the chain homogeneous transformations, we could derive the force vector with respect to any hand frame:

$$V = \prod_{i=1}^{n} {}_{i}^{i-1}T \cdot V_0, \tag{5}$$

where V and V_0 are homogeneous representation of 3-d vectors. In practice, we generate force vectors on each phalanx regarding wrist frame.

C. Visualization

To visualize the reconstructed hand motion, we create a hand model in ROS Unified Robot Description Format (URDF). In this model, we define the structure and connected joints of the human hand, as well as parameters such as the lengths of each phalanx and dimensions of the palm, which are measured in advance.

TABLE III: General standard Denavit-Hartenberg parameters of a finger

Link ID	α_{i-1}	a_{i-1}	θ_i	d_i
1	0	0	β	0
2	$\pi/2$	l_1	θ_1	0
3	0	l_2	θ_2	0
4	0	l_3	θ_3	0

TABLE IV: Concatenation of transformation matrices

Phalanx	Transformation
Proximal	${}_{1}^{0}T\,{}_{2}^{1}T$
Middle/Distal for thumb	${}_{1}^{0}T\,{}_{2}^{1}T\,{}_{3}^{2}T$
Distal	${}_{1}^{0}T\,{}_{2}^{1}T\,{}_{3}^{2}T\,{}_{4}^{3}T$

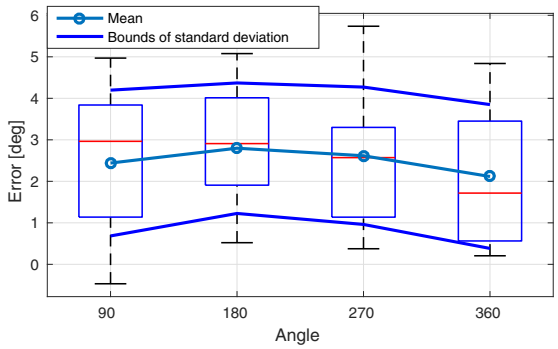

Fig. 6: Bias and standard deviation of an individual IMU with up to 360° rotation. Red horizontal lines indicate median error, and the bottom and top edges of the blue boxes indicate the 25th and 75th percentiles, respectively. The whiskers extend to the most extreme data points not considered outliers.

The orientation of each joint, as calculated in the forward kinematics, is then assigned to each linkage of the hand model to visualize the hand pose. We further create a set of force markers to indicate both the magnitude and direction of the forces being exerted by the palm and fingers over each of the 26 force sensing taxels, providing a visualization of the distribution of forces over the palm. Each finger proximal and distal link corresponds with one force marker while the palm link includes a 16-marker array which accords with the distribution of sensor grids on palm. The color of the marker remains green if the sensor is inactive, and turns red if force is applied.

IV. Performance Evaluation

We evaluate the performance of individual components as well as of the system as a whole. Three experiments are conducted. The bias and variance of an individual IMU are firstly obtained. We further examine the accuracy of reconstructing a static angle with two articulated IMUs, indicating the performance of basic element using the pose sensing approach in the actual setup. The Velostat force sensor is evaluated by the quality of the force response in grasping a bottle having different weights. Captured pose and force information are also jointly evaluated via force vector visualization. Lastly, we perform the tasks of opening three types of medicine bottles that require different sets of manipulative actions.

A. IMU Evaluation

a) Single IMU evaluation: As the reliability of the pose sensing critically relies upon the IMU performance, it is crucial to take the IMU's bias and variance into account, thus an experiment is conducted to model those quantities. An IMU is rotated driven by a precise stepper motor controlled by an Arduino microcontroller at a constant angular velocity of 60 RPM. Four rotation angles, 90°, 180°, 270°, and 360° are executed twenty times each. No rotating angles of

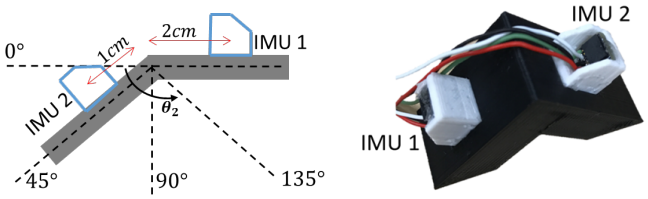

(a) Schematic of the setup (b) Actual exemplary setup

Fig. 7: Experimental setup for evaluating the angle reconstruction with two articulated IMUs

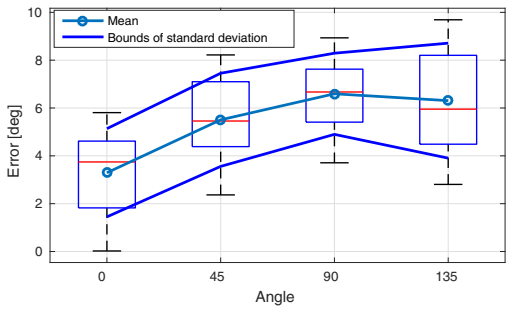

Fig. 8: Mean and standard deviation of the reconstructed angles using articulated IMUs under different angles including the boxplot of the collected data. Red horizontal lines indicate median error, and the bottom and top edges of the blue boxes indicate the 25th and 75th percentiles, respectively. The whiskers extend to the most extreme data points not considered outliers.

greater than 360° are necessary as it is far beyond fingers' rotation limits. Fig. 6 illustrates the mean and the standard deviation of the error of such rotating angles. The IMU displays consistent error characteristics, that is having a bias of 2° to 3° with a standard deviation of ±1.7°, with small variations for all 4 rotation angles. Such results indicate that the selected IMU is generally reliably within the applications of the proposed design.

b) Articulated IMU reconstruction of fixed angles: Based on the data of two adjacent IMUs that span a joint of interest, assuming revolute joint, we test the accuracy of the estimated joint angle. Four rigid bends with fixed angles of 0° 45°, 90°, and 135° are manufactured to simulate an rotation angle of a revolute joint. These four angles are selected since they evenly divide the reachable area of a finger joint with small exceeding based on Equation 2. The experimental schematic is shown in Fig. 7a. Fig. 7b is an exemplary setup using 90° joint angle: IMU 1 is placed 2cm away behind the bend, simulating the IMU attached to proximal phalanx, while IMU 2 is placed 1cm ahead of the bend, corresponding to the IMU on the middle phalanx. The IMU placement is identical to that in the prototype glove. For each bending angle, the test is repeated twenty times, and the joint angle estimates are shown in Fig. 8. As bending angles increase, the reconstructed angle errors increase from 4° to approximately 6° while the confidence intervals increase. We can see that articulated IMUs under-perform as the rotated angle increases, but the error range is still reasonable and the designed IMUs configuration can reliably fulfill the task.

B. Grasping Bottles

After establishing the force-voltage relation of the proposed Velostat force sensors, we evaluate the performance of the entire force sensor network as a whole by performing grasping action. The reason that we choose grasping is becuase it is one of the most common actions in manipulation. An experiment in grasping an *empty*, *half-full*, and *full* water bottle, whose weight is 0.13kg, 0.46kg, and 0.75kg, respectively, is conducted to demonstrate the capability in differentiating low, medium, and high grasping forces.

The grasping hand pose is shown in the Fig. 10a. The pose is natural and no artificial force is applied other than the force just sufficient to grasp and hold the bottle stably. For each bottle condition, ten grasps are performed. The force in the palm is treated as the average of the sixteen force readings from the 4-by-4 force sensor on the palm to simplify the analysis. Similarly, the force in each finger is the average of the 2-by-1 force sensor. More careful inspections of force exerted in grasping can also be proceeded by analyzing the response of every force sensing unit. The results shown in Fig. 9 indicate the force increments is correlated with the weight increments of the bottle.

Fig. 10b shows the visualization of the grasping pose and the force vector, which reliably captures the actual manipulative action. This experiment qualitatively indicates the sensitivity and reliability of the force sensing using proposed Velostat force sensors.

C. Capturing Fine Manipulative Actions

Using the prototype system, a series of manipulative actions in opening three types of medicine bottles are studied. Each bottle equips different lock mechanisms and requires particular actions for removing the bottle lid. *Bottle 1* has no safety lock and can be opened by simply twisting the lid. *Bottle 2* requires the lid to be simultaneously pressed down and twisted to open. *Bottle 3* requires pinching the lid's safety lock in order to open it. For *Bottle 2* and *Bottle 3*, some of the actions in the sequence (*i.e.* pressing and pinching) are hard to perceive without recovering the force exerted by the hand. In the first row of Fig. 11a, 11b, and 11c, we visualize the manipulative action sequences captured for opening *Bottle 1*, *Bottle 2*, and *Bottle 3*, respectively. The second row of each corresponding figure illustrates the actual action sequences captured by a RGB camera.

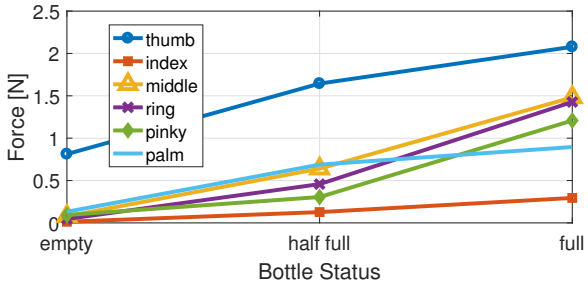

Fig. 9: Force response of grasping empty, half-full, and full bottles, respetively.

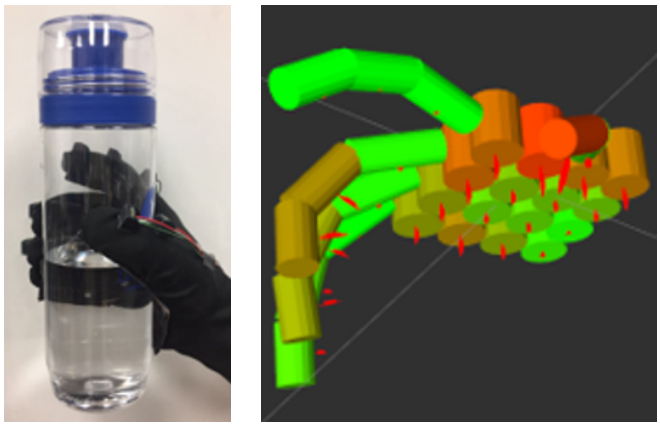

(a) Actual grasping pose (b) Force vector

Fig. 10: Grasp of half-full bottle and captured pose and force vector

Visualization: In contrast to the action sequences captured by a RGB camera, the visualization results provide additional force information regarding the different fine manipulative actions involved in the opening the bottles. For instance, the fingers in Fig. 11b are flat and parallel to the bottle lid, while the one in Fig. 11c is similar to gripping pose. The responses of force markers are also different due to varying contact points between the human hand and the lid: high responses in Fig. 11b are concentrated on palm area, while in Fig. 11c, there are only two evident responses on distal thumb and index finger. Without taking force responses into account, the actions sequences of opening *Bottle 1* and *Bottle 3* are very similar to each other (see Fig. 11a and 11c).

The capability of detecting the visually unobservable forces has been shown as one of the advantages of the proposed design in studying the fine manipulative actions. By analyzing the spatio-temporal signals of force and pose in terms of joint angles, we can also evaluate the performance of the design as a whole.

Data interpretation: Due to the distinct safety lock mechanisms equipped, the manipulative actions required for opening these three types of medicine bottles are different as shown in Fig. 11. The proposed glove-based system successfully captures the differences, and Fig. 12 illustrates the force collected at one taxel on palm and at the fingertip of thumb, as well as the flexion angle of the MCP joint of the index finger.

As opening the *Bottle 2* requires pressing the lid, the proposed system captures high force response on the palm area. In contrast, the other two bottles yields very low force response in the same region. If we look at the force exerted at the fingertip of the thumb, opening *Bottle 3* with pinch-to-open lock has larger force in magnitude and longer duration compared to opening *Bottle 1* as it comes with no safety lock and it only involves twisting the lid with mild force. The thumb does not contact with the lid in opening *Bottle 2*, yielding no force response.

For joint angle measurements, since opening both *Bottle 1* and *Bottle 3* involve similar twist action, the measured flexion angles of the MCP joint in the index finger are around 50°

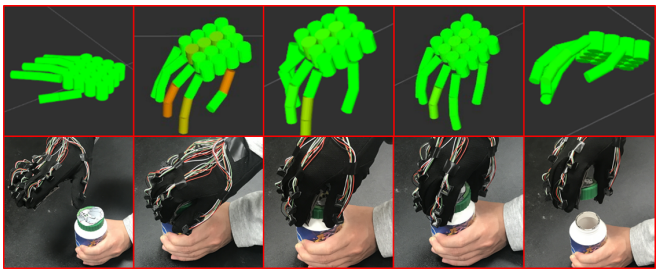

(a) *Bottle 1*, regular twist to open

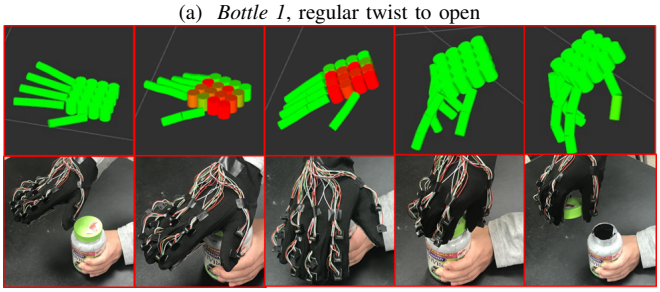

(b) *Bottle 2*. pressing the lid to open

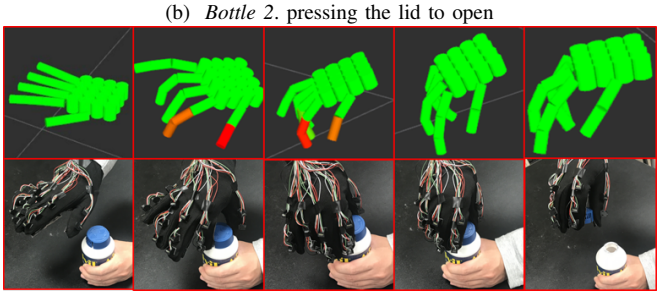

(c) *Bottle 3*, pinching lock to open

Fig. 11: Action sequences and visualizations of opening three types of bottles

in both cases. In opening *Bottle 2*, only the palm touches the lid and the fingers remain stretched, resulting in small flexion angle.

V. Conclusion and Future Work

We present a design of a glove-based system, capable of simultaneously collecting human hand pose and exerted contact force data during hand-object interaction with fine manipulative actions. The overall system design is firstly illustrated, following by the hardware implementations. In software implementation, we have defined the kinematic chain of a hand, in order to reconstruct the hand pose. Using custom Velostat force sensor taxels, we are able to measure the hand-object interaction forces across large regions of the hand. In the visualization framework, the simulated hand model successfully reflects subtle differences in grasping action sequences when interacting with three different types of bottles with various safety locks. By quantitatively analyzing the collected spatio-temporal signals of force and pose, we show the potentials using the proposed glove, as well as some preliminary analysis for studying hand-object dynamics. A direct application using the proposed system is to enable robot to learn and perform finer manipulative actions through human demonstrations [27]. Recent study also shows the haptic feedback is crucial for recognizing interactions [28], indicating potential applications in social interactions [29],

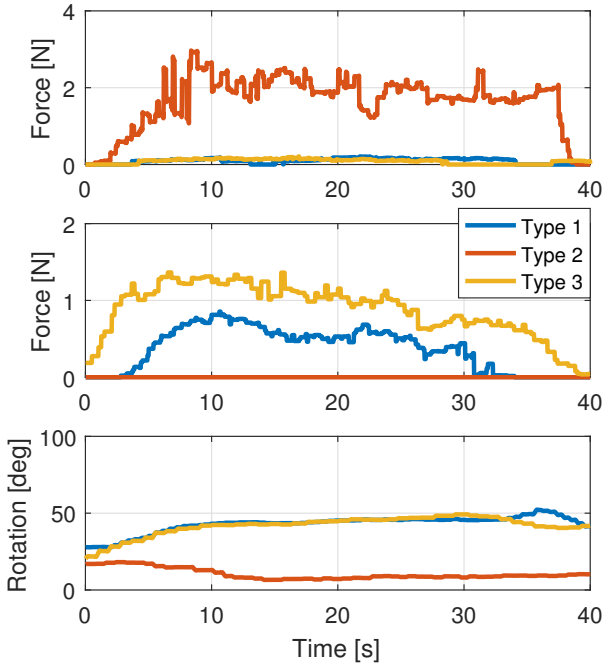

Fig. 12: Force signals captured in palm (top) and the fingertip of thumb (middle), and flexion angle of index finger's MCP joint (bottom).

[30].

In future, a potential direction would be improving the current kinematic modeling of the thumb to better reflect the actual structure and the DoF of the thumb. Some industrial manufacturing methods, such as laser cutting, could be introduced in fabricating and assembling the Velostat force sensor to achieve a more consistent performance.

Acknowledgement

We thank Yaofang Zhang of the UCLA Electrical Engineering Department, Eric Peltola, Alireza Fathaliyan, and Xiaoyu Wang of Biomechatronics Lab at UCLA Mechanical and Aerospace Engineering Department for useful discussions and assistance with experiments. We also thank Carl Turner for useful discussions and assistance with the PCB design. The work reported herein was supported by DARPA XAI grant N66001-17-2-4029, DARPA SIMPLEX grant N66001-15-C-4035 and ONR MURI grant N00014-16-1-2007 (to Zhu), and ONR grant N00014-16-1-2468 (to Santos).

References

[1] G. Tagne, P. Hénaff, and N. Gregori, "Measurement and analysis of physical parameters of the handshake between two persons according to simple social contexts," in *International Conference on Intelligent Robots and Systems (IROS)*, IEEE, 2016.

[2] A. Kleinsmith and N. Bianchi-Berthouze, "Affective body expression perception and recognition: A survey," *Transactions on Affective Computing*, vol. 4, no. 1, pp. 15–33, 2013.

[3] S. S. Rautaray and A. Agrawal, "Vision based hand gesture recognition for human computer interaction: a survey," *Artificial Intelligence Review*, vol. 43, no. 1, pp. 1–54, 2015.

[4] Y. Zhu, Y. Zhao, and S. Chun Zhu, "Understanding tools: Task-oriented object modeling, learning and recognition," in *Conference on Computer Vision and Pattern Recognition (CVPR)*, 2015.

[5] T.-H. Pham, A. Kheddar, A. Qammaz, and A. A. Argyros, "Towards force sensing from vision: Observing hand-object interactions to infer manipulation forces," in *Conference on Computer Vision and Pattern Recognition (CVPR)*, 2015.

[6] Y. Wang, J. Min, J. Zhang, Y. Liu, F. Xu, Q. Dai, and J. Chai, "Video-based hand manipulation capture through composite motion control," *ACM Transactions on Graphics (TOG)*, vol. 32, no. 4, p. 43, 2013.

[7] W. Zhao, J. Zhang, J. Min, and J. Chai, "Robust realtime physics-based motion control for human grasping," *ACM Transactions on Graphics (TOG)*, vol. 32, no. 6, p. 207, 2013.

[8] L. Dipietro, A. M. Sabatini, and P. Dario, "A survey of glove-based systems and their applications," *Transactions on Systems, Man, and Cybernetics, Part C (Applications and Reviews)*, vol. 38, no. 4, pp. 461–482, 2008.

[9] T. Taylor, S. Ko, C. Mastrangelo, and S. J. M. Bamberg, "Forward kinematics using imu on-body sensor network for mobile analysis of human kinematics," in *Engineering in Medicine and Biology Society (EMBC)*, IEEE, 2013.

[10] H. G. Kortier, V. I. Sluiter, D. Roetenberg, and P. H. Veltink, "Assessment of hand kinematics using inertial and magnetic sensors," *Journal of Neuroengineering and Rehabilitation*, vol. 11, no. 1, p. 70, 2014.

[11] G. Ligorio and A. M. Sabatini, "Extended kalman filter-based methods for pose estimation using visual, inertial and magnetic sensors: comparative analysis and performance evaluation," *Sensors*, vol. 13, no. 2, pp. 1919–1941, 2013.

[12] G. Santaera, E. Luberto, A. Serio, M. Gabiccini, and A. Bicchi, "Low-cost, fast and accurate reconstruction of robotic and human postures via imu measurements," in *International Conference on Robotics and Automation (ICRA)*, IEEE, 2015.

[13] H. G. Kortier, J. Antonsson, H. M. Schepers, F. Gustafsson, and P. H. Veltink, "Hand pose estimation by fusion of inertial and magnetic sensing aided by a permanent magnet," *Transactions on Neural Systems and Rehabilitation Engineering*, vol. 23, no. 5, pp. 796–806, 2015.

[14] R. K. Kramer, C. Majidi, R. Sahai, and R. J. Wood, "Soft curvature sensors for joint angle proprioception," in *International Conference on Intelligent Robots and Systems (IROS)*, IEEE, 2011.

[15] N. S. Kamel, S. Sayeed, and G. A. Ellis, "Glove-based approach to online signature verification," *Transactions on Pattern Analysis and Machine Intelligence (TPAMI)*, vol. 30, no. 6, pp. 1109–1113, 2008.

[16] I. Choi, E. W. Hawkes, D. L. Christensen, C. J. Ploch, and S. Follmer, "Wolverine: A wearable haptic interface for grasping in virtual reality," in *International Conference on Intelligent Robots and Systems (IROS)*, IEEE, 2016.

[17] F. L. Hammond, Y. Mengüç, and R. J. Wood, "Toward a modular soft sensor-embedded glove for human hand motion and tactile pressure measurement," in *International Conference on Intelligent Robots and Systems (IROS)*, IEEE, 2014.

[18] Y. Gu, W. Sheng, M. Liu, and Y. Ou, "Fine manipulative action recognition through sensor fusion," in *International Conference on Intelligent Robots and Systems (IROS)*, IEEE, 2015.

[19] E. Battaglia, M. Bianchi, A. Altobelli, G. Grioli, M. G. Catalano, A. Serio, M. Santello, and A. Bicchi, "Thimblesense: a fingertip-wearable tactile sensor for grasp analysis," *IEEE Transactions on Haptics*, vol. 9, no. 1, pp. 121–133, 2016.

[20] M. Mohammadi, T. L. Baldi, S. Scheggi, and D. Prattichizzo, "Fingertip force estimation via inertial and magnetic sensors in deformable object manipulation," in *Haptics Symposium (HAPTICS)*, IEEE, 2016.

[21] J. Low, P. Khin, and C. Yeow, "A pressure-redistributing insole using soft sensors and actuators," in *International Conference on Robotics and Automation (ICRA)*, IEEE, 2015.

[22] G. Pugach, A. Melnyk, O. Tolochko, A. Pitti, and P. Gaussier, "Touch-based admittance control of a robotic arm using neural learning of an artificial skin," in *International Conference on Intelligent Robots and Systems (IROS)*, IEEE, 2016.

[23] S. Müller, C. Schröter, and H.-M. Gross, "Smart fur tactile sensor for a socially assistive mobile robot," in *International Conference on Intelligent Robotics and Applications*, Springer, 2015.

[24] E. Jeong, J. Lee, and D. Kim, "Finger-gesture recognition glove using velostat (iccas 2011)," in *International Conference on Control, Automation and Systems (ICCAS)*, IEEE, 2011.

[25] B. W. Lee and H. Shin, "Feasibility study of sitting posture monitoring based on piezoresistive conductive film-based flexible force sensor," *Sensors*, vol. 16, no. 1, pp. 15–16, 2016.

[26] J. Lin, Y. Wu, and T. S. Huang, "Modeling the constraints of human hand motion," in *Workshop on Human Motion*, IEEE, 2000.

[27] M. Edmonds, F. Gao, X. Xie, H. Liu, S. Qi, Y. Zhu, B. Rothrock, and S.-C. Zhu, "Feeling the force: Integrating force and pose for fluent discovery through imitation learning to open medicine bottles," in *International Conference on Intelligent Robots and Systems (IROS)*, IEEE, 2017.

[28] T. Shu, S. Thurman, D. Chen, S. Zhu, and H. Lu, "Critical features of joint actions that signal human interaction," in *Proceedings of the 38th annual meeting of the cognitive science society*, 2016.

[29] T. Shu, X. Gao, M. S. Ryoo, and S.-C. Zhu, "Learning social affordance grammar from videos: Transferring human interactions to human-robot interactions," in *International Conference on Robotics and Automation (ICRA)*, IEEE, 2017.

[30] T. Shu, M. S. Ryoo, and S.-C. Zhu, "Learning social affordance for human-robot interaction," in *International Joint Conference on Artificial Intelligence (IJCAI)*, 2016.